chemengineering

MDPI

Article

Photocatalytic and Antimicrobial Properties of Ag_2O/TiO_2 Heterojunction

Maya Endo-Kimura [1], Marcin Janczarek [1,2,*], Zuzanna Bielan [1,3], Dong Zhang [1], Kunlei Wang [1], Agata Markowska-Szczupak [1,4] and Ewa Kowalska [1,*]

1 Institute for Catalysis, Hokkaido University, Sapporo 001-0021, Japan; m_endo@cat.hokudai.ac.jp (M.E.-K.); zuzanna.bielan@gmail.com (Z.B.); zhang.d@cat.hokudai.ac.jp (D.Z.); kunlei@cat.hokudai.ac.jp (K.W.); agata@erb.pl (A.M.-S.)
2 Institute of Chemical Technology and Engineering, Faculty of Chemical Technology, Poznan University of Technology, 60-965 Poznan, Poland
3 Department of Process Engineering and Chemical Technology, Gdansk University of Technology, 80-233 Gdansk, Poland
4 Institute of Chemical and Environmental Engineering, West Pomeranian University of Technology, Szczecin, Pulaskiego 10, 70-322 Szczecin, Poland
* Correspondence: marcin.janczarek@put.poznan.pl (M.J.); kowalska@cat.hokudai.ac.jp (E.K.)

Received: 5 December 2018; Accepted: 2 January 2019; Published: 8 January 2019

Abstract: Ag_2O/TiO_2 heterojunctions were prepared by a simple method, i.e., the grinding of argentous oxide with six different titania photocatalysts. The physicochemical properties of the obtained photocatalysts were characterized by diffuse-reflectance spectroscopy (DRS), X-ray powder diffraction (XRD) and scanning transmission electron microscopy (STEM) with an energy dispersive X-ray spectroscopy (EDS). The photocatalytic activity was investigated for the oxidative decomposition of acetic acid and methanol dehydrogenation under UV/vis irradiation and for the oxidative decomposition of phenol and 2-propanol under vis irradiation. Antimicrobial properties were tested for bacteria (*Escherichia coli*) and fungi (*Candida albicans* and *Penicillium chrysogenum*) under UV and vis irradiation and in the dark. Enhanced activity was observed under UV/vis (with synergism for fine anatase-containing samples) and vis irradiation for almost all samples. This suggests a hindered recombination of charge carriers by p-n heterojunction or Z-scheme mechanisms under UV irradiation and photo-excited electron transfer from Ag_2O to TiO_2 under vis irradiation. Improved antimicrobial properties were achieved, especially under vis irradiation, probably due to electrostatic attractions between the negative surface of microorganisms and the positively charged Ag_2O.

Keywords: heterogeneous photocatalysis; nanocomposites; heterojunction; Ag_2O; TiO_2; antimicrobial properties

1. Introduction

Recently, the application potential of semiconductor photocatalysis, related to environmental remediation and renewable energy processes [1], has been gaining importance in environmentally clean and future technologies [2–4]. Titanium(IV) oxide (TiO_2, titania) is an n-type semiconductor of great importance for applied photocatalysis [5–7]. The advantages of this material are an exceptional high photocatalytic efficiency, chemical inertness, long-term stability and photo-corrosion resistance. The current challenge for the development of technologies based on photocatalysis is still the design of TiO_2-originated material with high efficiency in both UV and visible light (vis) irradiation. It should be pointed out that titania is inactive in vis range due to its wide bandgap, and quantum yield under UV irradiation is much lower than 100%, due to the recombination of charge carriers (typical for all

semiconductors). Therefore, the introduction of vis absorption into titania and the hindering of charge carriers' recombination would enable its broad application also under natural sunlight. Therefore, the design of new photocatalysts based on TiO_2 should consider the above mentioned issues [8–11].

One of the main strategies to improve the performance of titania is its coupling with other semiconductors [12]. It is considered that the heterojunction of titania (n-type semiconductor) and p-type semiconducting material should result in an efficient charge separation, and thus, an increase in the lifetime of charge carriers [13]. To introduce the vis response, a p-type semiconductor with a lower bandgap energy than TiO_2 is necessary. A promising candidate for a narrow bandgap semiconductor to couple with TiO_2 is low-cost silver(I) oxide (Ag_2O, argentous oxide). The band gap energy of Ag_2O has been experimentally determined to be 1.3 ± 0.3 eV [14]. However, Ag_2O is not often used as a single photocatalyst, because it is unstable and photo-sensitive under light irradiation [15–18]. Furthermore, Ag_2O, with a body-centered cubic crystal structure (the same as in the case of Cu_2O), allows a large variety of particle morphologies to be synthesized [16,17,19,20]. Silver(I) oxide has also strong antibacterial properties, which might depend on the shape of Ag_2O particles [19].

The modification of titania with silver nanoparticles (NPs) or mixed silver forms (Ag(0), Ag^+, Ag^{2+}) to prepare photocatalysts has already been performed by many research groups [21–37]. However, in the case of Ag_2O/TiO_2 system, there are only a few research papers and the mechanism of the coupling is still not fully understood [38–49]. The consequence of the p-n heterojunction is the movement of the photogenerated electrons to the conduction band of n-type TiO_2 and the photogenerated holes to the valence band of p-type Ag_2O, which promotes an interfacial electron transfer causing the reduction of the charge recombination effect [42]. Different morphological forms of anatase were used to prepare Ag_2O/TiO_2, such as nanofibers [39,49], nanobelts [40,46], nanosheets [41] and microspheres [47]. Rutile [42,50] and P25 (highly active, commercial titania sample containing anatase (76–80%), rutile (13–15%) and amorphous phase (6–11%) [51]) [44,45] were also considered in these preparations. It is important to mention that in the majority of studies, organic dyes were used as test compounds to check photocatalytic activity, even in the vis range of irradiation, which is not an appropriate selection, due to the possibility of titania sensitization [52]. Moreover, there is a lack of complex discussion about the effect of the titania matrix on the efficiency of the Ag_2O/TiO_2 system. Therefore, in this study, the p-n heterojunction of Ag_2O and TiO_2 has been investigated for photocatalytic decomposition of organic compounds and the inactivation of microorganisms (bacteria and fungi) in dependence on the titania matrix (anatase, rutile and mixed-phase titania).

2. Materials and Methods

2.1. Preparation of Ag_2O/TiO_2 Photocatalysts

TiO_2 samples were supplied by several sources: P25 (AEROXIDE® TiO_2 P25, Nippon Aerosil, Tokyo, Japan), ST01, (ST-01, Ishihara Sangyo, Osaka, Japan) ST41 (ST-41, Ishihara Sangyo), TIO6 (TIO-6, Catalysis Society of Japan, Tokyo, Japan), RUT and RUT' (rutile nanopowder and predominantly rutile, Merck, Darmstadt, Germany). Ag_2O was supplied by Wako Pure Chemicals. All materials were used as received, without further processing. Ag_2O/TiO_2 composites were prepared by the physical mixing of Ag_2O and TiO_2 powders in an agate mortar, i.e., the titania sample was mixed with Ag_2O to prepare composites containing 1 wt% of Ag_2O (5, 10, and 50 wt% were also tested for some reactions). The time of grinding (5 min) was the same for all samples to ensure the appropriate uniformity of the prepared composite powders.

2.2. Characterization

The UV/vis diffuse reflectance spectra (DRS) were recorded on JASCO V-670 (JASCO, Tokyo, Japan), equipped with a PIN-757 integrating sphere, using $BaSO_4$ as a reference. Diffraction patterns (XRD) were collected on an X-ray diffractometer (Rigaku intelligent XRD SmartLab with a Cu target). The crystallite size was estimated by the diffraction peak using the Scherrer equation. The morphology

of samples and distribution of Ag_2O were observed by scanning transmission electron microscopy, equipped with an energy-dispersive X-ray spectroscopy (STEM-EDS, HD-2000, HITACHI, Tokyo, Japan). The content of silver was estimated by atomic absorption spectroscopy (AAS) after Ag dissolution from Ag_2O/TiO_2 in aqua regia.

2.3. Photocatalytic Activity Tests

The photocatalytic activities of the prepared photocatalysts were tested in four reaction systems: (1) Decomposition of acetic acid under UV/vis irradiation, (2) dehydrogenation of methanol under UV/vis irradiation, (3) decomposition of phenol under vis irradiation ($\lambda > 400$ nm: Xe lamp, water IR filter, cold mirror and cut-off filter L42), and (4) oxidation of 2-propanol ($\lambda > 420$ nm: Xe lamp, water IR filter, cold mirror and cut-off filter Y45). For the activity testing, 50 mg of photocatalyst was suspended in 5 mL of aqueous solution of (1) acetic acid (5 vol%), (2) methanol (50 vol%), (3) phenol (20 mg/L), and 2-propanol (5 vol%). The suspension for reaction (2) was bubbled with argon before irradiation. The 35-mL testing tubes were sealed with rubber septa, continuously stirred and irradiated in a thermostated water bath. Amounts of liberated (1) carbon dioxide in a gas phase, (2) hydrogen in a gas phase, (3) phenol, benzoquinone, and (4) acetone in a liquid phase (after powder separation; 0.3-mL sample was withdrawn for analysis) were determined by gas (GC-TCD (1-2), GC-FID (4)), and liquid (HPLC (3)) chromatography. The irradiation set-ups were described elsewhere [53]. In brief, the photoreactor for vis activity testing consisted of two parts (Figure 1). In the first part, light emitted from an Xe lamp (equipped with a cold mirror) passed through a water bath, and then through a removable UV cut-off filter (to eliminate IR and UV radiation, respectively). In the second part, two test-tubes were placed behind the filter at the same distance from the light source (4.5 cm × 4.5 cm—the irradiation window). Their contents were continuously stirred by magnetic stirrers and kept at a constant temperature by the thermostated water. To achieve the water circulation through the two parts (to avoid filter damage and to achieve constant reaction temperature) and to avoid UV light penetration into the second part, a separating wall was mounted in the first part parallel to the light beam. The cooling water was circulated over the separating wall and then through the hole at the bottom of the partition wall between the two parts. All inner parts of the reactor were covered with black tape and both parts were closed with metal covers. The light intensity measured in the front of the testing tubes (in the second part) was ca. 9.2 mW cm^{-2} and 11.3 mW cm^{-2} for reaction system (3) and (4), respectively.

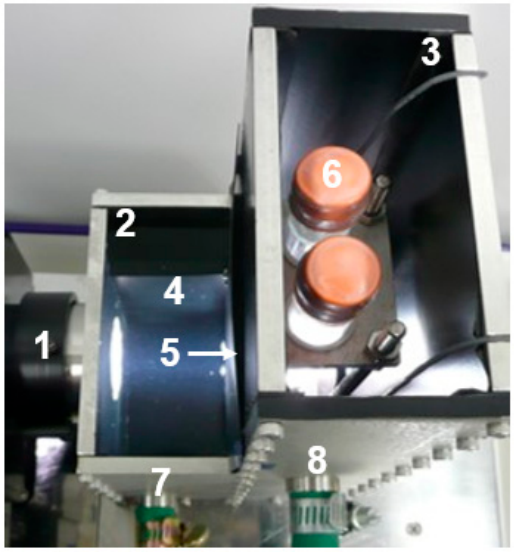

Figure 1. Photograph of photoreactor (top view): (1) Irradiation source (Xe lamp with cold mirror), (2) first part, (3) second part, (4) separating wall, (5) UV cut-off filter, (6) testing tube, (7) water inlet, (8) water outlet.

2.4. Bactericidal Activity Test

The bactericidal activity of the prepared samples was examined by the suspension method: 50 mg of samples (1 and 5 wt% Ag_2O/ST01, Ag_2O (2.5 mg; the same content as that in 5 wt% Ag_2O/ST01 sample) and bare ST-01) were dispersed in 7.0 mL of *Escherichia coli* K12 (*E. coli* K12, ATCC29425) suspension at a concentration of ca. 0.180 Abs at 630 nm (ca. 1–5 $\times$ 10^8 cells/mL) in a test tube and irradiated with an Xe lamp and a (i) CM1 and Y-45 filter for vis experiments ($\lambda > 420$ nm with ca. 20.0 mW·cm^{-2}), or (ii) CM2 and UV-D36B filter for UV experiments ($300 < \lambda < 420$ nm with ca. 1.1 mW·cm^{-2}) under continuous stirring in a thermostated water bath (photoreactor described in previous reports [53] and shown in Figure 1), or kept in the dark under stirring (500 rpm). The suspensions were diluted and aliquots of the suspensions were inoculated on a plate count agar (Becton, Dickinson and Company, Franklin Lakes, NJ, USA) at 0, 0.5, 1, 2, and 3 h. Media were incubated at 37 °C overnight and then the colonies were counted.

2.5. Fungicidal Activity Test

2.5.1. Suspension Method

50 mg of samples (1 and 5 wt% Ag_2O/ST01, Ag_2O and bare ST01) was dispersed in a test tube in 7.0 mL of *Candida albicans* (*C. albicans*, isolated from patients (throat smear) with immunodeficiency disorders that cause candidiasis (IIT&EE ZUT collection)) suspension at a concentration of ca. 0.400 Abs at 630 nm (ca. 1 $\times$ 10^4 cells/mL) and irradiated with UV and vis (same reactor and conditions as for bactericidal tests (2.4)) or kept in the dark under stirring (500 rpm). Serial dilutions were prepared, and aliquots of the suspensions were inoculated on sabouraud dextrose agar (Becton, Dickinson and Company, Franklin Lakes, NJ, USA) media at 0, 0.5, 1, 2 and 3 h. Media were incubated at 37 °C overnight and then the colonies were counted.

2.5.2. Spore Counting Method

20 g/L of the samples (1 and 5 wt% Ag_2O/ST01 and bare ST01) and 0.2 g/L and 1.0 g/L of Ag_2O (corresponding to Ag_2O amount in 1 and 5 wt% Ag_2O/ST-01, respectively) in Malt Extract Agar (Merck, Darmstadt, Germany) were autoclaved at 121 °C for 10 min, and the agar slants were prepared. Spores of *Penicillium chrysogenum* (*P. chrysogenum*) were suspended in 8.5 g/L NaCl aqueous solution, 20 µL of 10,000 spores/µL suspension was inoculated on the agar slants and irradiated with fluorescence light (FL) or kept in the dark for 5 days. After cultivation, spores were collected with 0.05% triton X-100 in 8.5 g/L NaCl aqueous solution by vortex mixing. Spore suspensions were diluted 10 or 50 times with 8.5 g/L NaCl aqueous solution and counted.

3. Results and Discussion

3.1. Characterization of Ag_2O/TiO_2 Samples

Six titania samples, which are commercially available, i.e., anatase-predominant samples (ST01 and ST41), rutile-predominant samples (TIO6, RUT and RUT') and mixed-phase titania (P25), were used for the preparation of silver(I) oxide/titania nanocomposites. Crystalline properties, i.e., content and crystallite size of obtained photocatalysts are shown in Table 1.

Ag_2O was detected in all coupled samples (Table 1 and Figure 2), and its content varied depending on the titania used (from 0.1 to 0.7 wt%). Such varieties in the Ag_2O content are quite reasonable considering that only 1 wt% of Ag_2O was used for titania modification (low-content modifiers are quite often undetectable). The crystallite sizes of titania (anatase and rutile) practically did not change after grinding (original sizes reported previously [6]). In contrast, the crystallite size of Ag_2O decreased from about 60 nm to even 3 nm, resulting from the lower hardness of Ag_2O [54] than that of titania. Interestingly, it was found that the change in Ag_2O size corelated with TiO_2 crystallite sizes, i.e., the smaller the crystallites of TiO_2 were, the larger was a decrease in the Ag_2O size after grinding.

Moreover, the exact content of silver was confirmed in the Ag_2O/ST01 sample (for 5 wt% of Ag_2O, i.e., 4.65 wt% of Ag) by AAS reaching 4.66 wt% and 4.60 wt% of Ag for solid and suspended (for precipitate; same suspension as that used for photocatalytic activity tests) samples, respectively.

Table 1. Properties of Ag_2O/TiO_2 photocatalysts.

Sample Name	Crystalline Content * (%)			Crystallite Size (nm)		
	Anatase	Rutile	Ag_2O	Anatase	Rutile	Ag_2O
Ag_2O/P25	82.5	16.9	0.6	21.8	38.5	18.3
Ag_2O/ST01	99.9	-	0.1	7.8	-	3.2
Ag_2O/ST41	99.6	-	0.4	75.7	-	7.8
Ag_2O/TiO6	7.3	92.2	0.5	6.3	15.9	13.0
Ag_2O/RUT	2.0	97.4	0.6	38.9	86.1	29.8
Ag_2O/RUT′	11.5	87.4	0.7	109.2	170.1	41.3
Ag_2O	-	-	100	-	-	58.7

* Crystalline composition without consideration of amorphous phase.

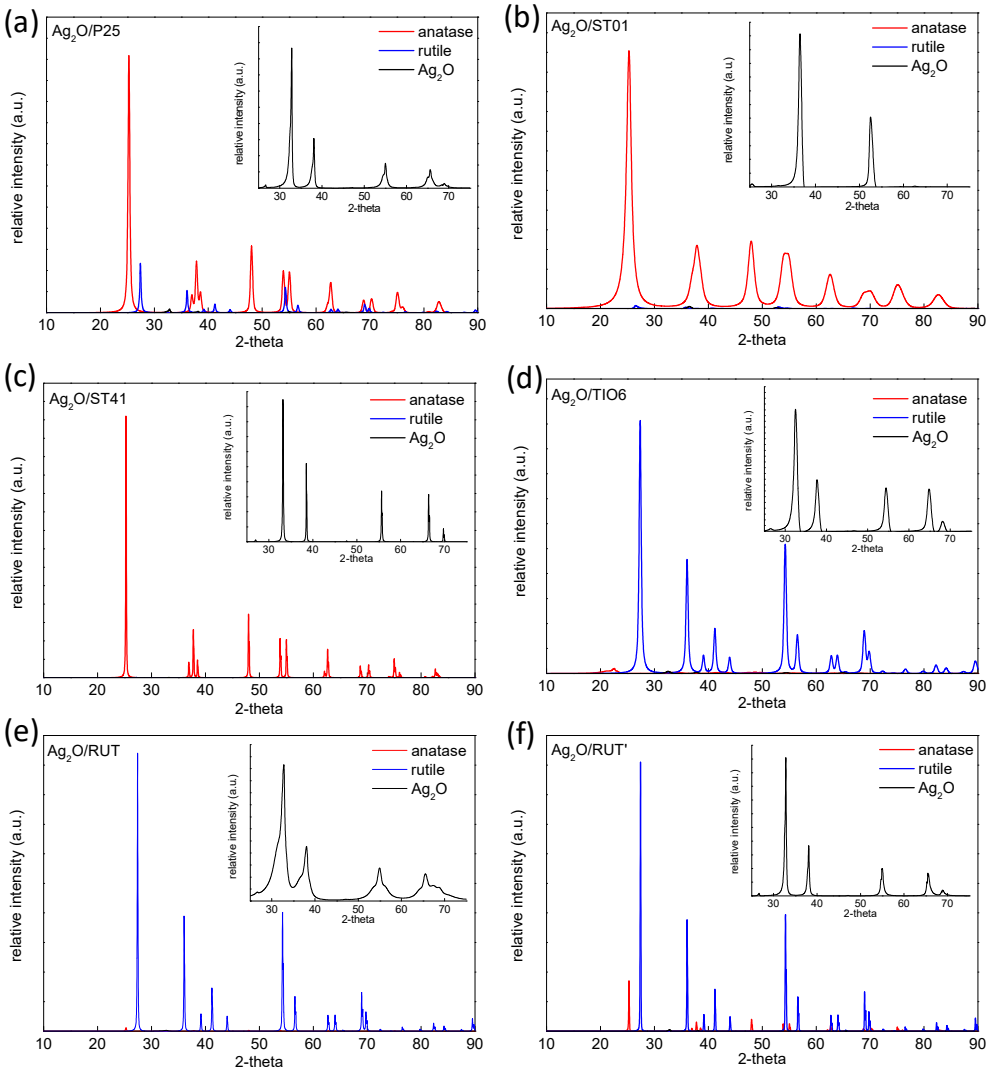

Figure 2. XRD diffractograms of Ag_2O/TiO_2 samples: (**a**) Ag_2O/P25, (**b**) Ag_2O/ST01, (**c**) Ag_2O/ST41, (**d**) Ag_2O/TIO6, (**e**) Ag_2O/RUT, (**f**) Ag_2O/RUT′. (Insets) XRD patterns of Ag_2O (after subtraction of titania peaks).

Diffuse reflectance spectra (DRS) of the obtained composites and exemplary DRS of bare titania (ST41) and Ag_2O are shown in Figure 3. Titania can only absorb UV light, and depending on its polymorphic form (anatase vs. rutile) a different absorption edge is observed, i.e., bathochromic shift for rutile samples is caused by its narrower bandgap. Silver oxide is black, and thus can absorb all photons in entire range of 200–800 nm with maximum at ca. 500–550 nm, which corresponds to 2.25-eV bandgap [55]. After the titania grinding with Ag_2O, the absorption at vis range appeared with different intensities and positions of its maximum (500–700 nm) depending on the titania.

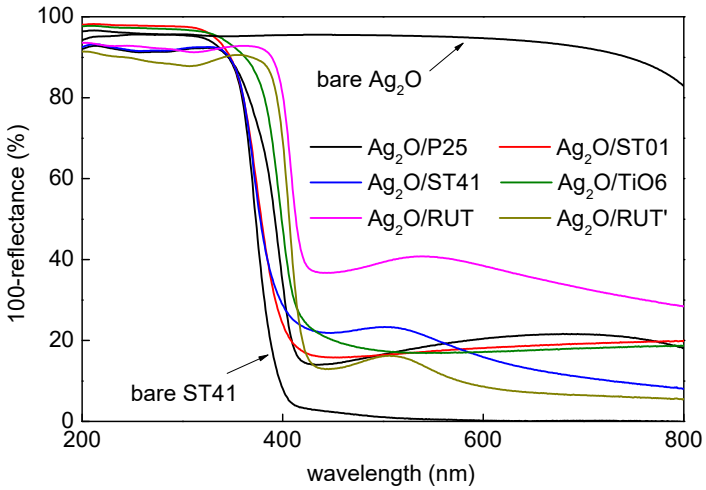

Figure 3. Diffuse reflectance spectra of Ag_2O/TiO_2 samples.

Exemplary STEM (with EDS mapping) images of Ag_2O/ST01 sample are shown in Figure 4. It was found that indeed NPs of Ag_2O were much smaller ($\leq$15 nm) than that used for the sample preparation, confirming the XRD results (Table 1). Ag_2O deposits (nano-sized and NPs) were uniformly distributed on the titania matrix. Additionally, atomic percentages of oxygen, titanium and silver (64.1%, 34.2% and 1.8%) confirmed that stable p-n heterojunction could be prepared by simple grinding.

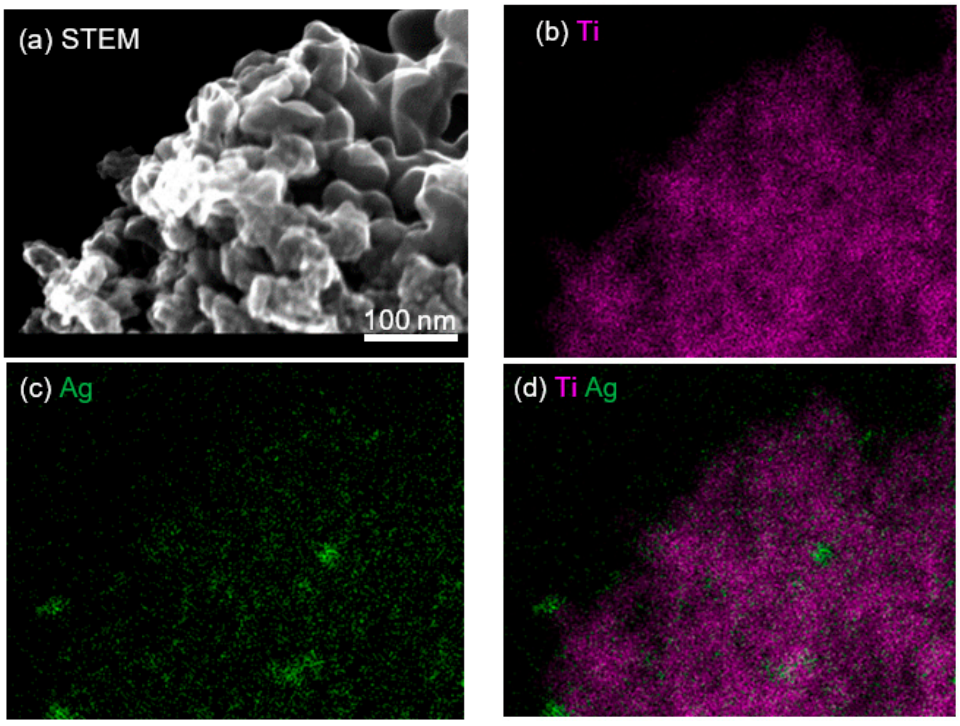

Figure 4. STEM (**a**) and EDS (Ti- (**b**), Ag (**c**) and merge of Ti and Ag (**d**)) images of Ag_2O/ST01.

3.2. Photocatalytic Activity

3.2.1. UV/Vis-Induced Methanol Dehydrogenation

Photocatalytic activity was investigated under UV/vis irradiation for two reactions: (i) Methanol dehydrogenation under anaerobic conditions (H_2 system), and (ii) decomposition of acetic acid under aerobic conditions (CO_2 system; discussed in the next section (Section 3.2.2)). Obtained data of methanol dehydrogenation are shown in Figure 5.

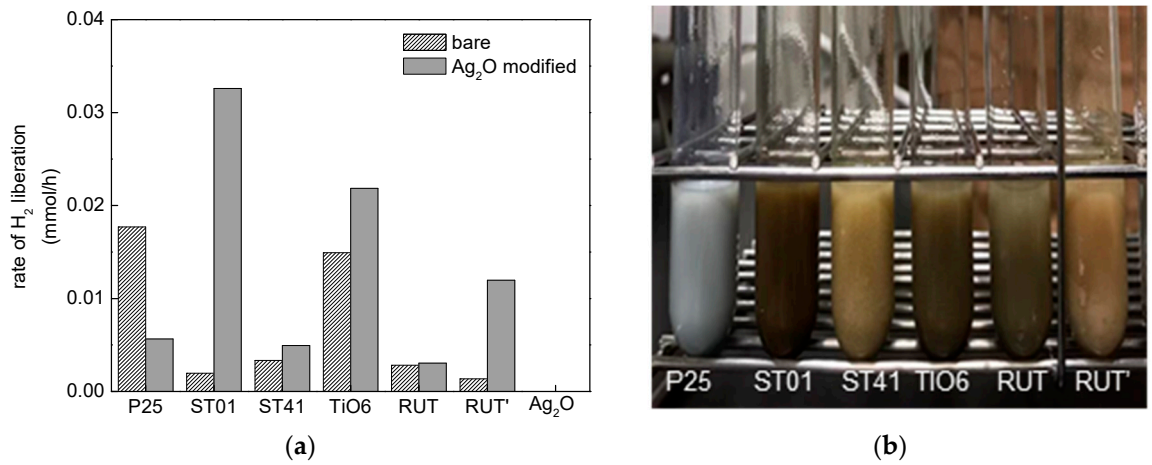

Figure 5. UV/vis photocatalytic efficiency of Ag_2O/TiO_2 samples with a different titania matrix in methanol dehydrogenation reaction (**a**) with respective photographs of samples after 45-min irradiation (**b**).

At first, the influence of the Ag_2O content was tested for the Ag_2O/ST01 sample in the H_2 system, and it was found that 1 wt% resulted in the highest level of photocatalytic activity, e.g., an increase in the Ag_2O content from 1 to 10 wt% resulted in a decrease in photocatalytic activity by ca. half, probably due to the inner-filter effect (significant darkening of irradiated suspension). Therefore, for further studies, the composites containing 1 wt% of Ag_2O were used.

For almost all the samples, the addition of inactive Ag_2O to titania caused a significant increase in H_2 liberation. The most active system with an obvious synergistic effect was Ag_2O/ST01, where the addition of 1 wt% of Ag_2O enhanced the reaction rate over 30 times. The only exception was the P25 matrix, where activity suddenly decreased after grinding with Ag_2O. P25 was also used as a titania base by Ren et al. [56], where it was shown that a too high content of Ag_2O (above 5 wt%) caused a drop in photocatalytic activity during the methyl orange degradation. Possible reactions for the heterojunction Ag_2O/TiO_2 system in methanol dehydrogenation under deaerated conditions are presented below.

$$TiO_2 + h\nu \rightarrow e^- + h^+$$

$$Ag_2O + h\nu \rightarrow e^- + h^+$$

$$CH_3OH + 2h^+ \rightarrow HCHO + 2H^+$$

$$H^+ + e^- \rightarrow 0.5\,H_2$$

$$Ag^+ + e^- \rightarrow Ag$$

Under UV/vis irradiation both semiconductors (TiO_2 and Ag_2O) are excited, which causes the generation of charge carriers, i.e., electrons and holes. Methanol works as a hole scavenger to hinder the hole-electron recombination. Therefore, photogenerated electrons can easily reduce protons, resulting in hydrogen formation. It is proposed that the enhanced photocatalytic activity by heterojunction between two oxides might be caused by a Z-scheme mechanism resulting in more reductive properties

of Ag_2O/TiO_2 than that of bare TiO_2 (more negative CB of Ag_2O than that of TiO_2). Figure 6 presents the possible mechanism of methanol dehydrogenation. Considering the darkening of suspension during irradiation (right parts of Figure 5 vs. Figure 7) in highly reductive conditions (anaerobic, methanol, UV), it is proposed that Ag_2O was reduced forming zero-valent silver deposits (+1.17 V vs. SHE) being the co-catalyst for hydrogen evolution [22–24,57].

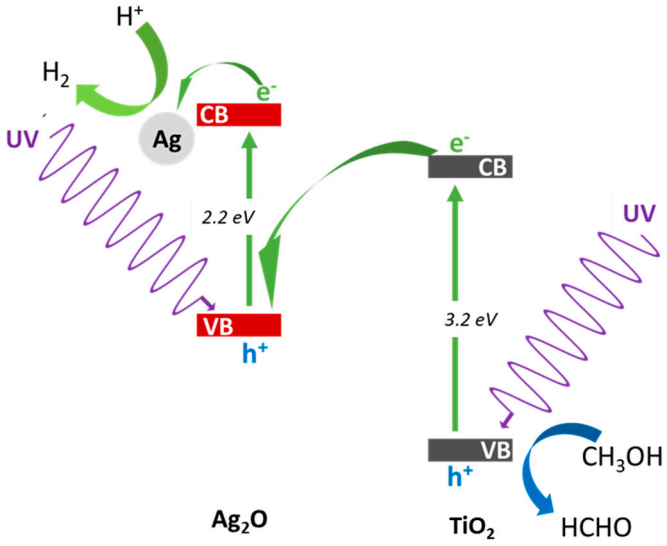

Figure 6. The schematic mechanism of Z-scheme for UV/vis-induced methanol dehydrogenation with $Ag(0)/Ag_2O/TiO_2$ photocatalysts.

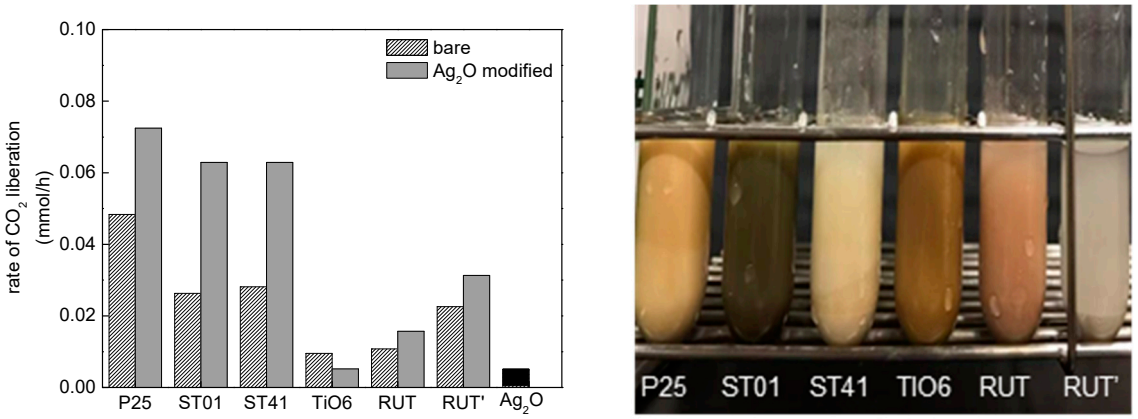

(**a**) (**b**)

Figure 7. UV/vis photocatalytic efficiency of Ag_2O/TiO_2 samples with a different titania matrix in acetic acid oxidation (**a**) with respective photographs of samples after 45-min irradiation (**b**).

3.2.2. UV/Vis-Induced Acetic Acid Oxidation

The photocatalytic activity of the obtained Ag_2O/TiO_2 photocatalysts was also measured in an acetic acid oxidative decomposition reaction. The obtained rates of the CO_2 generation are presented in Figure 7.

As a reference material, bare Ag_2O was also tested, and it was found that Ag_2O was almost inactive also for CO_2 liberation. For almost all Ag_2O/TiO_2 composites, the photocatalytic activity was much higher than that by the respective bare TiO_2 samples. Two-times improvement was reached for anatase-predominant samples (ST01 and ST41). It is proposed that through similarity to another heterojunction system Cu_2O/TiO_2 [58], two kinds of mechanisms could be proposed, i.e., Z-scheme and p-n heterojunction (II type), as shown in Figure 8. The first mechanism (recombination between e^- (TiO_2) and h^+ (Ag_2O)) is preferential for high photocatalytic activity, due to the high oxidation

(h^+ in titania) and reduction (e^- in argentous oxide) potential of the obtained composites. It should be pointed out that the photocatalytic activity of the oxidation reactions depends on the oxidation potential of holes, and anatase has been reported as a stronger oxidant than rutile [59]. Therefore, the higher activities of Ag_2O/anatase than Ag_2O/rutile could be explained by the more positive position of its valence band (VB) [60]. Accordingly, the more negative potential of the conduction band (CB) in rutile than that in anatase might result in the formation of a II type heterojunction (e^- migration from CB of Ag_2O to CB of TiO_2 and an opposite migration of VB h^+) with less redox potential (CB of titania and VB of argentous oxide).

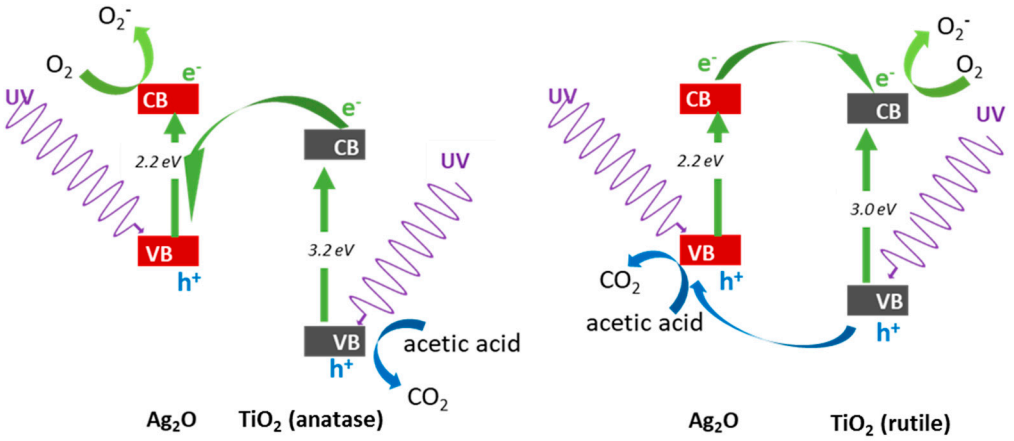

Figure 8. The schematic mechanisms of oxidative decomposition of acetic acid under UV/vis irradiation with Ag_2O/TiO_2 photocatalysts: Z-scheme for anatase (**a**) and heterojunction (type II) for rutile (**b**).

3.2.3. Visible Light Photocatalytic Activity

The vis photocatalytic activity of the obtained Ag_2O/TiO_2 composites was investigated for two reactions: (1) Oxidative decomposition of phenol and (2) oxidation of 2-propanol. Obtained data are shown in Figures 9 and 10.

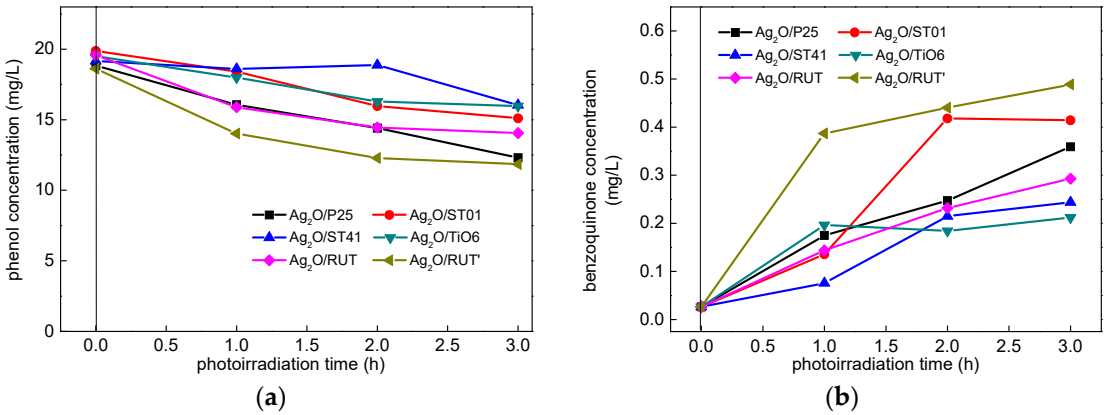

Figure 9. Change in phenol (**a**) and benzoquinone (**b**) concentrations during vis irradiation ($\lambda > 400$ nm) of Ag_2O/TiO_2 photocatalysts.

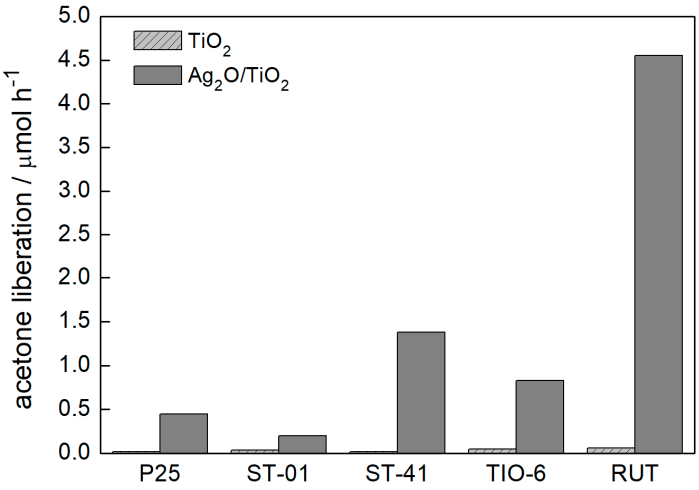

Figure 10. Vis (λ > 420 nm) photocatalytic activity of Ag_2O/TiO_2 photocatalysts for 2-propanol oxidation.

Under vis irradiation, titania was inactive due to its wide bandgap, and thus only argentous oxide could absorb photons, and indeed exhibited high vis activity. It was found that the modification of vis-inactive titania with argentous oxide resulted in the appearance of a vis response for all titania samples. The highest vis activity was found for rutile samples. It is proposed that the higher activity of rutile-containing samples could be caused by the lower redox potential of the excited rutile (more negative CB) than that of anatase [59,60] facilitating electron migration from excited Ag_2O to CB of titania, as shown in Figure 11. Buchalska et al. observed a more efficient $O_2^{\bullet -}$ generation on rutile than that on anatase, and thus a higher activity for photo-reactions involving photo-generated electrons as the predominant mechanism pathway. Consequently, higher activities of rutile than anatase have already been found for different vis systems, such as (1) plasmonic photocatalysts of gold-modified titania with "hot" (plasmonic) electron transfer from gold to CB of titania [53], and (2) Cu_2O/TiO_2 heterojunctions with an electron transfer from CB of cuprous oxide to CB of titania [61]. Nonetheless, the activity of bare argentous oxide was higher than that by Ag_2O/TiO_2 photocatalysts (1 h of irradiation was sufficient for the complete decomposition of phenol) confirming that Ag_2O with a narrow bandgap [49,61] was more vis active than TiO_2 and Ag_2O/TiO_2. Bare argentous oxide was not stable and could not be recycled after reaction, and thus, could not be treated as a "(photo)catalyst" (Similar results showing higher activity of Ag_2O than its composites with TiO_2 have already been published by Ren et al. [56] and Zhou et al. [40].). Therefore, it is concluded that the formation of Ag_2O/TiO_2 heterojunctions resulted in the preparation of more stable photocatalysts with high activity at a broad range of irradiation (UV and vis).

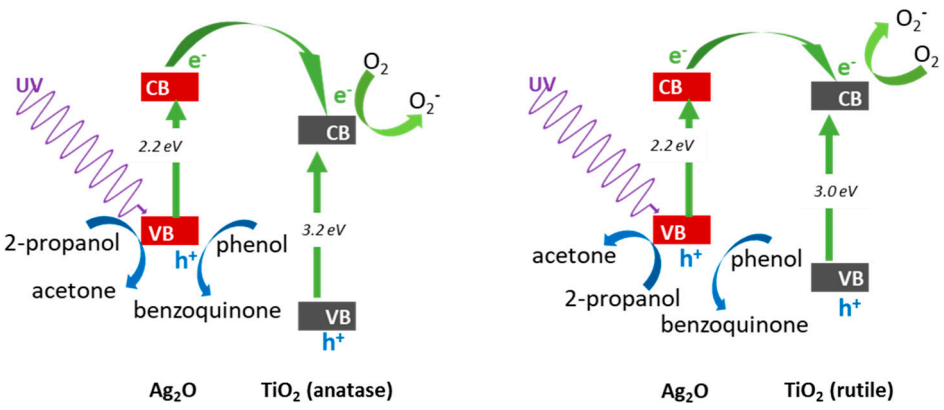

Figure 11. The schematic mechanisms of oxidative decomposition of 2-propanol and phenol under vis irradiation with Ag_2O/TiO_2 photocatalysts for anatase (**a**) and rutile (**b**).

3.3. Antimicrobial Properties of Ag_2O/TiO_2

It is widely known that silver cations possess high antimicrobial activity against various microorganisms, such as gram-negative/positive bacteria, fungi and protozoa. There are two main mechanisms of bactericidal activity of Ag^+, i.e., (i) the damage of the bacterial membrane [62], and (ii) deactivation of cellular enzymes [63], due to the high affinity of Ag^+ for bacterial membrane (negatively charged) and thiol groups of enzymes. Additionally, bactericidal activity of Ag_2O has recently been reported [64–66]. For example, it was proposed that chitosan-poly vinyl pyrrolidone-silver oxide nanoparticles possess higher bactericidal effect against gram-positive bacteria than gram-negative ones [14].

Figure 12 shows the bactericidal activity of Ag_2O/ST01, bare Ag_2O and bare TiO_2 (ST01) under UV, vis, and in the dark. It was found that bare titania was active only under UV irradiation, confirming that generated oxygen species could decompose bacterial cells. The highest antibacterial activity was observed for bare argentous oxide, similar to all tested conditions. In the cases of 1 wt% and 5 wt% Ag_2O/ST01, the order of activities was vis > UV > dark. Moreover, it was found that the activities of 5 wt% Ag_2O/ST01 were higher than those of 1 wt% Ag_2O/ST01 in all conditions. Thus, it is suggested that the high activity is directly correlated with the amount of Ag_2O. Moreover, considering that the large amount of Ag was released from the photocatalyst surface (66, 68, and 78% under vis, dark and UV, respectively), it is proposed that the dissolved Ag could attribute to the overall activity. The worse dark activity of Ag_2O/ST01 than that by bare Ag_2O could be caused by the hindered contact between bacteria and Ag_2O when TiO_2 partly covered its surface (interface decrease). However, it is clear that both UV and vis irradiation increased antibacterial activity, confirming the positive effect of photocatalysis. It is proposed that under vis irradiation, Ag_2O is excited with the simultaneous electron transfer to CB of titania resulting in either: (i) Positively charged Ag_2O (could be considered as local state) and its easier adsorption on bacterial cells, (ii) generation of ROS on TiO_2, (iii) direct oxidation by positive holes from VB of Ag_2O. Under UV irradiation, two mechanisms of photocatalysis could be considered, i.e., Z-scheme and p-n heterojunction (already discussed for photocatalytic oxidation of acetic acid). Considering the worse activity under UV than that under vis irradiation, the Z-scheme mechanism (for anatase/argentous oxide) seems more probable as the p-n junction should result in more positively charged Ag_2O (electron transfer from CB of Ag_2O to CB of TiO_2 and hole transfer from VB of TiO_2 to VB of Ag_2O), and thus higher activity than that in vis would be expected.

Antifungal activities were tested by two methods, i.e., suspension method (yeast *C. albicans*) and spore counting method (filamentous *P. chrysogenum*). Figure 13 shows the survival ratio of *C. albicans* on Ag_2O/ST01, Ag_2O and TiO_2 under UV, vis and in the dark in suspension method. Similarly, to bactericidal effect, bare Ag_2O was the most active independently on applied conditions (little higher activity: UV > dark > vis). Bare titania was only slightly active under UV irradiation (confirming Yang et al. study that *Candida* sp. were sensitive to photocatalysis [67]), and Ag_2O/ST01 was active only at higher content of argentous oxide (5 wt%) suggesting that Ag_2O was responsible for antifungal effect. Dark activity of Ag_2O/ST01 (5 wt%) was much lower than that of bare Ag_2O, probably due to decreased interface Ag_2O-fungus as titania partly covered argentous oxide. However, significant increase in activity was observed under vis irradiation confirming that direct contact between fungal cells and argentous oxide is a key-factor for high antifungal effect (under vis irradiation Ag_2O would be positively charged because of an electron transfer to CB of titania). In contrast, a decrease in activity under UV irradiation could confirm Z-scheme mechanism resulting in electron-rich Ag_2O surface (under UV irradiation both semiconductors would be excited with CB(TiO_2) electron and VB(Ag_2O) hole recombination leaving CB(Ag_2O) electrons and VB(TiO_2) holes). It has been reported that cell walls of *C. albicans* are negatively charged [68], and thus the repulsion between fungus and photocatalyst could be detrimental for antifungal activity.

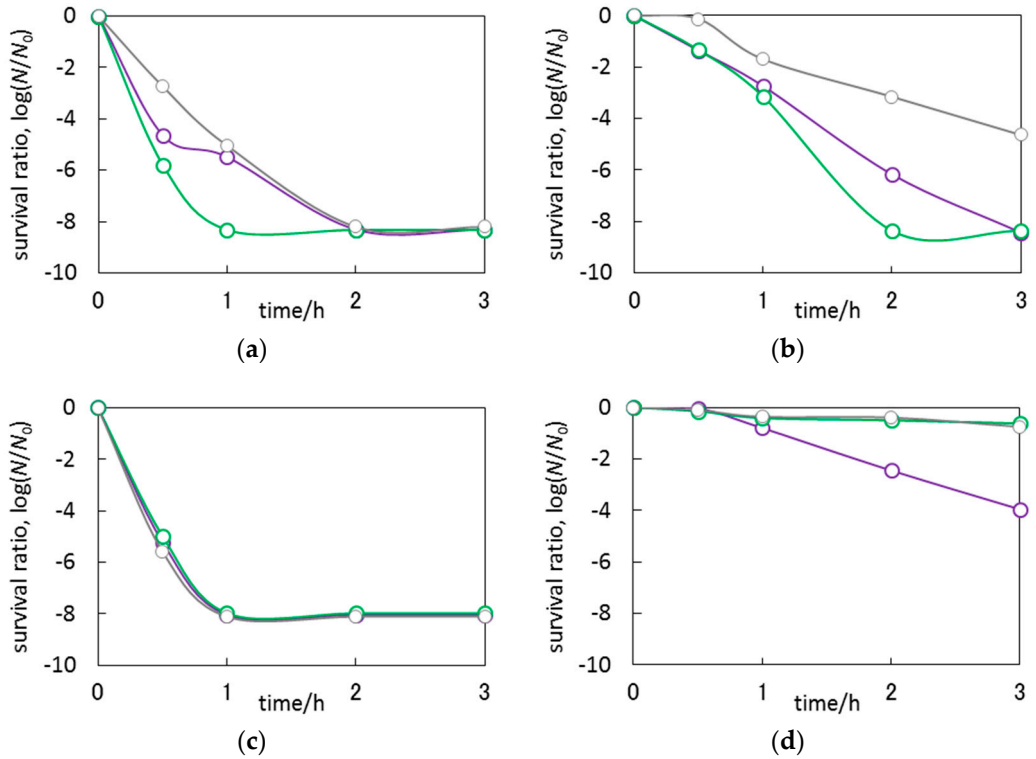

Figure 12. Survival ratio of *E. coli* K12 bacteria in the presence of 5 wt% Ag_2O/ST01 (**a**), 1 wt% Ag_2O/ST01 (**b**), Ag_2O (**c**) and bare ST01 (**d**) under UV irradiation (purple, 300 < λ < 420 nm), vis irradiation (green, λ > 420 nm), and in the dark (grey).

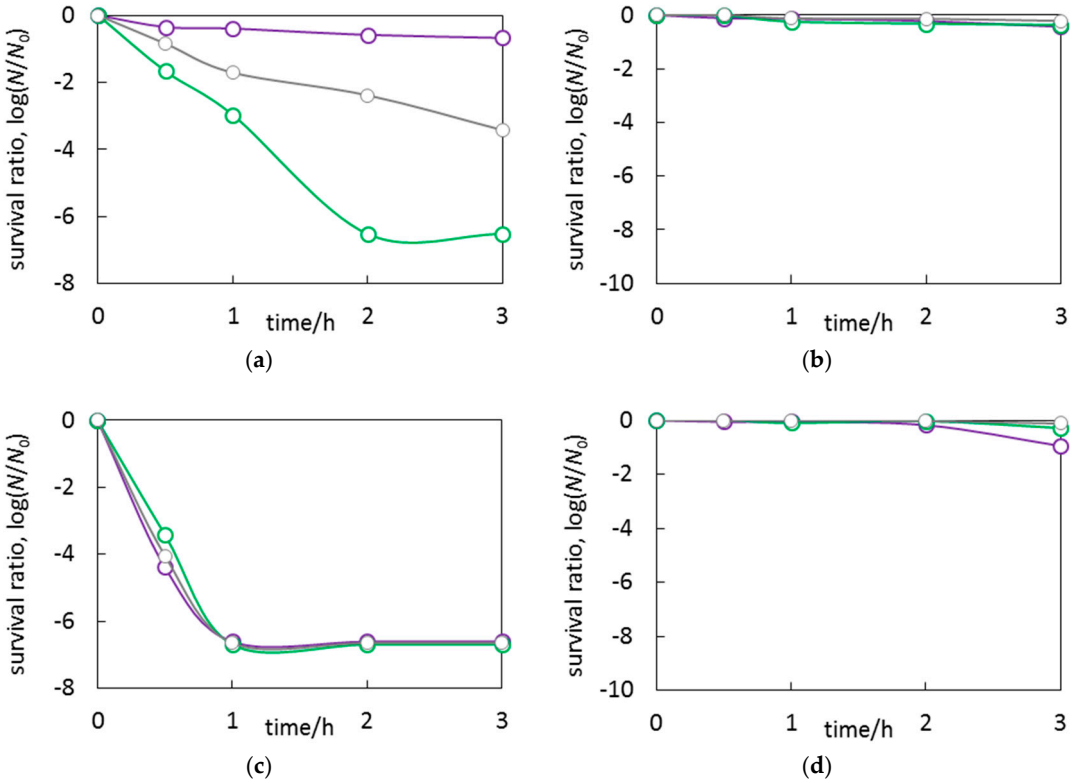

Figure 13. Survival ratio of *C. albicans* in the presence of 5 wt% Ag_2O/ST01 (**a**), 1 wt% Ag_2O/ST01 (**b**), Ag_2O (**c**) and bare ST01 (**d**) under UV irradiation (purple, 300 < λ < 420 nm), vis irradiation (green, λ > 420 nm), and in the dark (grey).

Fungicidal activity against *P. chrysogenum* was investigated by the spore-counting method (Figure 14). Both Ag_2O/ST01 samples (1 and 5 wt%) remarkably inhibited the generation of spores, and the formation of mycelium under fluorescence light (FL). Whereas, in contrast to yeast fungi and bacteria, the activity of bare Ag_2O was negligible (difficulty in Ag_2O adsorption on fungi in agar). In addition, 1 wt% Ag_2O/ST01 suppressed the growth of mycelium more efficiently than 5 wt% Ag_2O/ST01 under FL, corresponding to the photocatalytic activity of methanol dehydrogenation where the highest activity was obtained for the 1 wt% Ag_2O/ST01 sample. Therefore, it is proposed that the enhanced photocatalytic activity inhibited the fungal growth. However, samples in the dark showed higher activity than irradiated ones, especially bare ST01, in spite of the growth of mycelium. It should be pointed out that the number of spores formed in the control sample under FL was larger than that in the dark, since the light stimulated (was required for) fungal growth and sporulation [69–72]. It was reported that filamentous (mold) fungi showed a high variability (depending on the strain and place of isolation) in the reaction with titania, light, and combined titania/light [72,73]. It should be also taken into consideration that titania might enhance the growth of plants. Both the plant and fungus kingdom share many characteristic, such as the nucleus and cell organelles enclosed within membranes, cell walls made of cellulose, lack of ability to move and thread-like structures (fungal and plant roots) [74]. Therefore, in the case of ST01, it is proposed that the coexistence of titania and light accelerates the fungal growth (growth stimulation>photocatalytic activity).

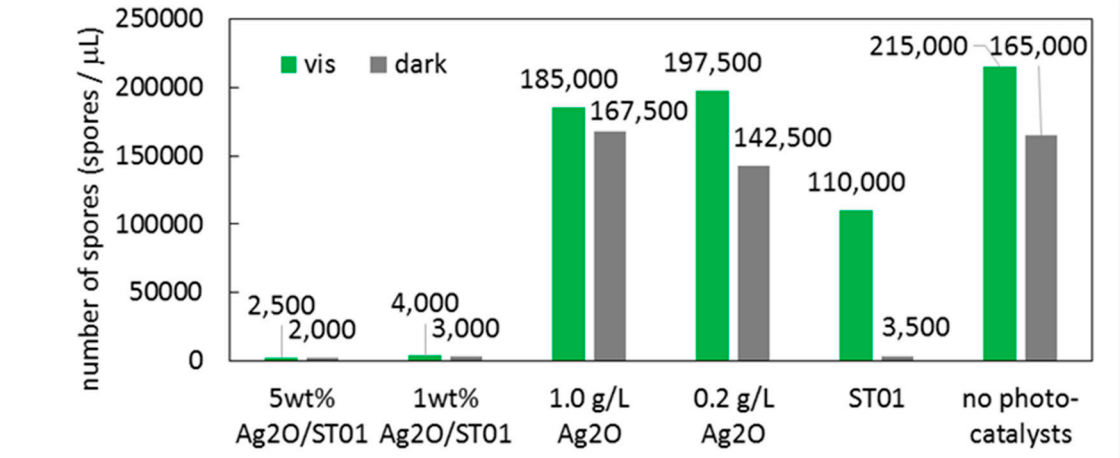

(**a**)

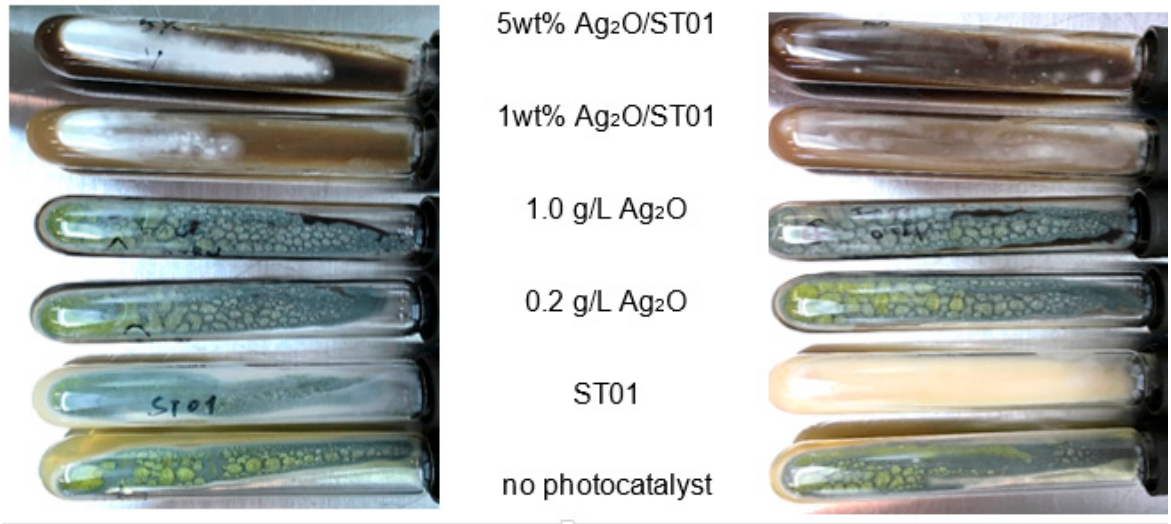

(**b**) (**c**)

Figure 14. Sporulation after five days growth of *P. chrysogenum* under florescence light and in the dark (**a**) and representative photographs of slants under florescence light (**b**) and in the dark (**c**).

4. Summary and Conclusions

In summary, a hybrid photocatalyst was prepared by a simple and cheap method, i.e., the grinding of silver(I) oxide and titania. The application of different kinds of titania photocatalysts allowed the preparation of samples significantly differed by resultant properties, and thus photocatalytic activities. It was found that although grinding did not change the crystal form of composites, titania crushed large particles/crystallites of Ag_2O, resulting in the formation of uniformly mixed composites.

A large improvement of photocatalytic activities was observed under UV/vis irradiation for methanol dehydrogenation and acetic acid oxidation. Two kinds of mechanisms could be responsible for this activity enhancement, i.e., Z-scheme and p-n junction. It is proposed that the mechanism might differ depending on the crystalline composition. For example, p-n junction could be more probable for the rutile-containing composite with a more negative CB level.

Additionally, it was found that titania modified with only 1 wt% of Ag_2O achieved a vis response by being active for the oxidative decomposition of phenol and 2-propanol. The composites containing rutile showed higher vis activity (similarly to previously reported plasmonic photocatalysts (Au/TiO_2) and Cu_2O/TiO_2 photocatalysts) suggesting that the more negative position of rutile CB could facilitate an electron transfer from vis-excited Ag_2O.

Ag_2O/TiO_2 photocatalysts exhibited high antimicrobial activities. Although antibacterial and anti-yeast activity was mainly caused by Ag_2O presence, independently on applied conditions (UV, vis and dark), antifungal activity for mold fungi was mainly caused by Ag_2O/TiO_2 composites. It was found that vis irradiation could significantly improve antibacterial and anti-yeast activities, due to the electrostatic attraction between the negative surface of microorganisms and the positively charged Ag_2O (after electron transfer to titania).

Author Contributions: M.J. and E.K. conceived and designed the experiments; M.E.-K., M.J., Z.B., A.M.-S. and E.K. interpreted the data and wrote the paper; M.E.-K. performed the antimicrobial tests and STEM/EDS; K.W. and D.Z. performed XRD, DRS and photocatalytic experiments; D.Z. prepared samples; K.W. drew the schematic mechanisms. All authors read, corrected, and approved the final version of manuscript.

Funding: The research was founded in part by the (i) Fusion Emergent Research project by the MEXT program of Integrated Research Consortium on Chemical Sciences (IRCCS), (ii) Institute for Catalysis, Hokkaido University (HU) within the framework of the research cluster on Plasmonic Photocatalysis, and (iii) Innovation Program for Foreign Professors (HU).

Acknowledgments: The authors thank Bunsho Ohtani for sound advice and unlimited access to laboratory equipment and Maxime Berry for his assistance in the preliminary study. M. J. acknowledges Hokkaido University for the guest lecturer position (2016–2017).

Conflicts of Interest: The authors declare no conflict of interest.

References

1. Hoffmann, M.R.; Martin, S.T.; Choi, W.Y.; Bahnemann, D.W. Environmental applications of semiconductor photocatalysis. *Chem. Rev.* **1995**, *95*, 69–96. [CrossRef]
2. Abe, R.; Higashi, M.; Domen, K. Overall water splitting under visible light through a two-step photoexcitation between TaON and WO_3 in the presence of an iodate-iodide shuttle redox mediator. *ChemSusChem* **2011**, *4*, 228–237. [CrossRef] [PubMed]
3. Fujishima, A.; Rao, T.N.; Tryk, D.A. Titanium dioxide photocatalysis. *J. Photochem. Photobiol. C Photochem. Rev.* **2000**, *1*, 1–21. [CrossRef]
4. Fattakhova-Rohlfing, D.; Zaleska, A.; Bein, T. Three-dimensional titanium dioxide nanomaterials. *Chem. Rev.* **2014**, *114*, 9487–9558. [CrossRef] [PubMed]
5. Fujishima, A.; Honda, K. Electrochemical photolysis of water at a semiconductor electrode. *Nature* **1972**, *238*, 37–38. [CrossRef] [PubMed]
6. Ohtani, B.; Mahaney, O.O.P.; Amano, F.; Murakami, N.; Abe, R. What are titania photocatalysts? An exploratory correlation of photocatalytic activity with structural and physical properties. *J. Adv. Oxid. Technol.* **2010**, *13*, 247–261. [CrossRef]

7. D'Oliveira, J.-C.; Al-Sayyed, G.; Pichat, P. Photodegradation of 2- and 3-chlorophenol in TiO_2 aqueous suspensions. *Environ. Sci. Technol.* **1990**, *24*, 990–996. [CrossRef]
8. Kisch, H. Semiconductor photocatalysis—Mechanistic and synthetic aspects. *Angew. Chem. Int. Ed.* **2013**, *52*, 812–847. [CrossRef]
9. Pelaez, M.; Nolan, N.T.; Pillai, S.C.; Seery, M.K.; Falaras, P.; Kontos, A.G.; Dunlop, P.S.M.; Hamilton, J.W.J.; Byrne, J.A.; O'Shea, K.; et al. A review on the visible light active titanium dioxide photocatalysts for environmental applications. *Appl. Catal. B Environ.* **2012**, *125*, 331–349. [CrossRef]
10. Schneider, J.; Matsuoka, M.; Takeuchi, M.; Zhang, J.; Horiuchi, Y.; Anpo, M.; Bahnemann, D.W. Understanding TiO_2 photocatalysis: Mechanisms and materials. *Chem. Rev.* **2014**, *114*, 9919–9986. [CrossRef]
11. Byrne, J.A.; Dunlop, P.S.M.; Hamilton, J.W.J.; Fernandez-Ibanez, P.A.; Polo-Lopez, I.; Sharma, P.K.; Vennard, A.S.M. A review of heterogeneous photocatalysis for water and surface disinfection. *Molecules* **2015**, *20*, 5574–5615. [CrossRef] [PubMed]
12. Kowalska, E.; Wei, Z.; Janczarek, M. Band-gap engineering of photocatalysts: Surface modification versus doping. In *Visible-Light-Active Photocatalysis: Nanostructured Catalyst Design, Mechanisms and Applications*; Ghosh, S., Ed.; Wiley: Weinheim, Germany, 2018; pp. 449–484.
13. Wang, H.; Zhang, L.; Chen, Z.; Hu, J.; Li, S.; Wang, Z.; Liu, J.; Wang, X. Semiconductor heterojunction photocatalysts: Design, construction, and photocatalytic performances. *Chem. Soc. Rev.* **2014**, *43*, 5234–5244. [CrossRef] [PubMed]
14. Tjeng, L.H.; Meinders, M.B.J.; Elp, J.; Ghijsen, J.; Sawatzky, G.A.; Johnson, R.L. Electronic structure of Ag_2O. *Phys. Rev. B* **1990**, *41*, 3190–3199. [CrossRef]
15. Wang, X.; Li, S.; Yu, H.; Yu, J.; Liu, S. Ag_2O as a new visible-light photocatalyst: Self-stability and high photocatalytic activity. *Chem. Eur. J.* **2011**, *17*, 7777–7780. [CrossRef] [PubMed]
16. Wang, G.; Ma, X.; Huang, B.; Cheng, H.; Wang, Z.; Zhan, J.; Qin, X.; Zhang, X.; Dai, Y. Controlled synthesis of Ag_2O microcrystals with facet-dependent photocatalytic activities. *J. Mater. Chem.* **2012**, *22*, 21189–21194. [CrossRef]
17. Chen, Y.J.; Chiang, Y.W.; Huang, M.H. Synthesis of diverse Ag_2O crystals and their facet-dependent photocatalytic activity examination. *ACS Appl. Mater. Interfaces* **2016**, *8*, 19672–19679. [CrossRef] [PubMed]
18. Jiang, W.; Wang, X.; Wu, Z.; Yue, X.; Yuan, S.; Lu, H.; Liang, B. Silver oxide as superb and stable photocatalyst under visible and near-infrared light irradiation and its photocatalytic mechanism. *Ind. Eng. Chem. Res.* **2014**, *54*, 832–841. [CrossRef]
19. Wang, X.; Wu, H.F.; Huang, R.B.; Xie, Z.X.; Zheng, L.S. Shape-dependent antibacterial activities of Ag_2O polyhedral particles. *Langmuir* **2010**, *26*, 2774–2778. [CrossRef] [PubMed]
20. Lyu, L.M.; Huang, M.H. Investigation of relative stability of different facets of Ag_2O nanocrystals through face-selective etching. *J. Phys. Chem. C* **2011**, *115*, 17768–17773. [CrossRef]
21. Wodka, D.; Bielanska, E.; Socha, R.P.; Elzbieciak-Wodka, M.; Gurgul, J.; Nowak, P.; Warszynski, P.; Kumakiri, I. Photocatalytic activity of titanium dioxide modified by silver nanoparticles. *ACS Appl. Mater. Interfaces* **2010**, *2*, 1945–1953. [CrossRef]
22. Kowalska, E.; Wei, Z.; Karabiyik, B.; Herissan, A.; Janczarek, M.; Endo, M.; Markowska-Szczupak, A.; Remita, H.; Ohtani, B. Silver-modified titania with enhanced photocatalytic and antimicrobial properties under UV and visible light irradiation. *Catal. Today* **2015**, *252*, 136–142. [CrossRef]
23. Janczarek, M.; Wei, Z.; Endo, M.; Ohtani, B.; Kowalska, E. Silver- and copper-modified decahedral anatase titania particles as visible light-responsive plasmonic photocatalyst. *J. Photonics Energy* **2017**, *7*, 012008. [CrossRef]
24. Wei, Z.; Janczarek, M.; Endo, M.; Colbeau-Justin, C.; Ohtani, B.; Kowalska, E. Silver-modified octahedral anatase particles as plasmonic photocatalyst. *Catal. Today* **2018**, *310*, 19–25. [CrossRef] [PubMed]
25. Zhang, H.; Wang, G.; Chen, D.; Lv, X.; Li, J. Tuning photoelectrochemical performances of Ag-TiO_2 nanocomposites via reduction/oxidation of Ag. *Chem. Mater.* **2008**, *20*, 6543–6549. [CrossRef]
26. Priya, R.; Baiju, K.V.; Shukla, S.; Biju, S.; Reddy, M.L.P.; Patil, K.; Warrier, K.G.K. Comparing ultraviolet and chemical reduction techniques for enhancing photocatalytic activity of silver oxide/silver deposited nanocrystalline anatase titania. *J. Phys. Chem. C* **2009**, *113*, 6243–6255. [CrossRef]
27. Kang, J.G.; Sohn, Y. Interfacial nature of Ag nanoparticles supported on TiO_2 photocatalysts. *J. Mater. Sci.* **2012**, *47*, 824–832. [CrossRef]

28. Liu, C.; Cao, C.; Luo, X.; Luo, S. Ag-bridged Ag_2O nanowire network/TiO_2 nanotube array p–n heterojunction as a highly efficient and stable visible light photocatalyst. *J. Hazard. Mater.* **2015**, *285*, 319–324. [CrossRef]
29. Cui, Y.; Ma, Q.; Deng, X.; Meng, Q.; Cheng, X.; Xie, M.; Li, X.; Cheng, Q.; Liu, H. Fabrication of Ag-Ag_2O/reduced TiO_2 nanophotocatalyst and its enhanced visible light driven photocatalytic performance for degradation of diclofenac solution. *Appl. Catal. B Environ.* **2017**, *206*, 136–145. [CrossRef]
30. Grabowska, E.; Zaleska, A.; Sorgues, S.; Kunst, M.; Etcheberry, A.; Colbeau-Justin, C.; Remita, H. Modification of titanium(IV) dioxide with small silver nanoparticles: Application in photocatalysis. *J. Phys. Chem. C* **2013**, *117*, 1955–1962. [CrossRef]
31. Mendez-Medrano, M.G.; Kowalska, E.; Lehoux, A.; Herissan, A.; Ohtani, B.; Bahena, D.; Briois, V.; Colbeau-Justin, C.; Rodriguez-Lopez, J.; Remita, H. Surface modification of TiO_2 with Ag nanoparticles and CuO nanoclusters for applications in photocatalysis. *J. Phys. Chem. C* **2016**, *120*, 5143–5154. [CrossRef]
32. Zielinska, A.; Kowalska, E.; Sobczak, J.W.; Lacka, I.; Gazda, M.; Ohtani, B.; Hupka, J.; Zaleska, A. Silver-doped TiO_2 prepared by microemulsion method: Surface properties, bio- and photoactivity. *Sep. Purif. Technol.* **2010**, *72*, 309–318. [CrossRef]
33. Sclafani, A.; Herrmann, J.-M. Influence of metallic silver and of platinum-silver bimetallic deposits on the photocatalytic activity of titania (anatase and rutile) in organic and aqueous media. *J. Photochem. Photobiol. A* **1998**, *113*, 181–188. [CrossRef]
34. Herrmann, J.M.; Tahiri, H.; AitIchou, Y.; Lassaletta, G.; GonzalezElipe, A.R.; Fernandez, A. Characterization and photocatalytic activity in aqueous medium of TiO_2 and Ag-TiO_2 coatings on quartz. *Appl. Catal. B Environ.* **1997**, *13*, 219–228. [CrossRef]
35. Sclafani, A.; Mozzanega, M.N.; Pichat, P. Effect of silver deposits on the photocatalytic activity of titanium dioxide samples for the dehydrogenation or oxidation of 2-propanol. *J. Photochem. Photobiol. A* **1991**, *59*, 181–189. [CrossRef]
36. Ohtani, B.; Kakimoto, M.; Miyadzu, H.; Nishimoto, S.; Kagiya, T. Effect of surface-adsorbed 2-propanol on the photocatalytic reduction of silver and/or nitrate ions in acidic TiO_2 suspensions. *J. Phys. Chem.* **1988**, *92*, 5773–5777. [CrossRef]
37. Nishimoto, S.; Ohtani, B.; Kajiwara, H.; Kagiya, T. Photoinduced oxygen formation and silver metal deposition in aqueous solutions of various silver salts by suspended titanium dioxide powder. *J. Chem. Soc. Faraday Trans. 1 Phys. Chem. Condens. Phases* **1983**, *79*, 2685–2694. [CrossRef]
38. Lalitha, K.; Reddy, J.K.; Sharma, M.V.P.; Kumari, V.D.; Subrahmanyam, M. Continuous hydrogen production activity over finely dispersed Ag_2O/TiO_2 catalysts from methanol:water mixtures under solar irradiation: A structure–activity correlation. *Int. J. Hydrogen Energy* **2010**, *35*, 3991–4001. [CrossRef]
39. You, Y.; Wan, L.; Zhang, S.; Xu, D. Effect of different doping methods on microstructure and photo-catalytic activity of Ag_2O–TiO_2 nanofibers. *Mater. Res. Bull.* **2010**, *45*, 1850–1854. [CrossRef]
40. Zhou, W.; Liu, H.; Liu, D.; Du, G.; Cui, J. Ag_2O/TiO_2 nanobelts heterostructure with enhanced ultraviolet and visible photocatalytic activity. *ACS Appl. Mater. Interfaces* **2010**, *2*, 2385–2392. [CrossRef]
41. Chen, F.; Liu, Z.; Liu, Y.; Fang, P.; Dai, Y. Enhanced adsorption and photocatalytic degradation of high-concentration methylene blue on Ag_2O-modified TiO_2-based nanosheet. *Chem. Eng. J.* **2013**, *221*, 283–291. [CrossRef]
42. Sarkar, D.; Ghosh, C.K.; Mukherjee, S.; Chattopadhyay, K.K. Three dimensional Ag_2O/TiO_2 Type-II (p−n) nanoheterojunctions for superior photocatalytic ctivity. *ACS Appl. Mater. Interfaces* **2013**, *5*, 331–337. [CrossRef] [PubMed]
43. Jiang, B.; Jiang, L.; Shi, X.; Wang, W.; Li, G.; Zhu, F.; Zhang, D. Ag_2O/TiO_2 nanorods heterojunctions as a strong visible-light photocatalyst for phenol treatment. *J. Sol-Gel Sci. Technol.* **2015**, *73*, 314–321. [CrossRef]
44. Ren, H.T.; Jia, S.Y.; Zou, J.J.; Wu, S.H.; Han, X. A facile preparation of Ag_2O/P25 photocatalyst for selective reductionof nitrate. *Appl. Catal. B Environ.* **2015**, *176*, 53–61. [CrossRef]
45. Sadanandam, G.; Kumari, V.D.; Scurrell, M.S. Highly stabilized Ag_2O-loaded nano TiO_2 for hydrogen production from glycerol: Water mixtures under solar light irradiation. *Int. J. Hydrogen Energy* **2016**, *42*, 807–820. [CrossRef]
46. Wei, N.; Cui, H.; Song, Q.; Zhang, L.; Song, X.; Wang, K.; Zhang, Y.; Li, J.; Wen, J.; Tian, J. Ag_2O nanoparticle/TiO_2 nanobelt heterostructures with remarkable photo-response and photocatalytic properties under UV, visible and near-infrared irradiation. *Appl. Catal. B Environ.* **2016**, *198*, 83–90. [CrossRef]

47. Liu, B.; Mu, L.; Han, B.; Zhang, J.; Shi, H. Fabrication of TiO_2/Ag_2O heterostructure with enhanced photocatalytic and antibacterial activities under visible light irradiation. *Appl. Surf. Sci.* **2017**, *396*, 1596–1603. [CrossRef]
48. Zelekew, O.A.; Kuo, D.H.; Yassin, J.M.; Ahmed, K.E.; Abdullah, H. Synthesis of efficient silica supported TiO_2/Ag_2O heterostructured catalyst with enhanced photocatalytic performance. *Appl. Surf. Sci.* **2017**, *410*, 454–463. [CrossRef]
49. Liu, G.; Wang, G.; Hu, Z.; Su, Y.; Zhao, L. Ag_2O nanoparticles decorated TiO_2 nanofibers as a p-n heterojunction for enhanced photocatalytic decomposition of RhB under visible light irradiation. *Appl. Surf. Sci.* **2019**, *465*, 902–910. [CrossRef]
50. Jiang, B.; Hou, Z.; Tian, C.; Zhou, W.; Zhang, X.; Wu, A.; Tian, G.; Pan, K.; Ren, Z.; Fu, H. A facile and green synthesis route towards two-dimensional TiO_2@Ag heterojunction structure with enhanced visible light photocatalytic activity. *Cryst. Eng. Commun.* **2013**, *15*, 5821–5827. [CrossRef]
51. Wang, K.L.; Wei, Z.S.; Ohtani, B.; Kowalska, E. Interparticle electron transfer in methanol dehydrogenation on platinum-loaded titania particles prepared from P25. *Catal. Today* **2018**, *303*, 327–333. [CrossRef]
52. Yan, X.; Ohno, T.; Nishijima, K.; Abe, R.; Ohtani, B. Is methylene blue an appropriate substrate for a photocatalytic activity test? A study with visible-light responsive titania. *Chem. Phys. Lett.* **2006**, *429*, 606–610. [CrossRef]
53. Kowalska, E.; Mahaney, O.O.P.; Abe, R.; Ohtani, B. Visible-light-induced photocatalysis through surface plasmon excitation of gold on titania surfaces. *Phys. Chem. Chem. Phys.* **2010**, *12*, 2344–2355. [CrossRef] [PubMed]
54. Souri, D.; Honarvar, F.; Tahan, Z.E. Characterization of semiconducting mixed electronic-ionic TeO_2-V_2O_5-Ag_2O glasses by employing ultrasonic measurements and Vicker's microhardness. *J. Alloys Compd.* **2017**, *699*, 601–610. [CrossRef]
55. Peyser, L.A.; Vinson, A.E.; Bartko, A.P.; Dickson, R.M. Photoactivated fluorescence from individual silver nanoclusters. *Science* **2001**, *291*, 103–106. [CrossRef]
56. Ren, H.T.; Yang, Q. Fabrication of Ag_2O/TiO_2 with enhanced photocatalytic performances for dye pollutants degradation by a pH-induced method. *Appl. Surf. Sci.* **2017**, *396*, 530–538. [CrossRef]
57. Wei, Z.; Endo, M.; Wang, K.; Charbit, E.; Markowska-Szczupak, A.; Ohtani, B.; Kowalska, E. Noble metal-modified octahedral anatase titania particles with enhanced activity for decomposition of chemical and microbiological pollutants. *Chem. Eng. J.* **2017**, *318*, 121–134. [CrossRef]
58. Janczarek, M.; Endo, M.; Zhang, D.; Wang, K.; Kowalska, E. Enhanced photocatalytic and antimicrobial prformance of cuprous oxide/titania: The effect of titania matrix. *Materials.* **2018**, *11*, 2069. [CrossRef]
59. Buchalska, M.; Kobielusz, M.; Matuszek, A.; Pacia, A.; Wojtyla, S.; Macyk, W. On oxygen activation at rutile- and anatase-TiO_2. *ACS Catal.* **2015**, *5*, 7424–7431. [CrossRef]
60. Scanlon, D.O.; Dunnill, C.W.; Buckeridge, J.; Shevlin, S.A.; Logsdail, A.J.; Woodley, S.M.; Catlow, C.R.A.; Powell, M.J.; Palgrave, R.G.; Parkin, I.P.; et al. Band alignment of rutile and anatase TiO_2. *Nat. Mater.* **2013**, *12*, 798–801. [CrossRef]
61. Allen, J.P.; Scanlon, D.O.; Watson, G.W. Electronic structures of silver oxides. *Phys. Rev. B* **2011**, *84*, 115141. [CrossRef]
62. Lok, C.N.; Ho, C.M.; Chen, R.; He, Q.Y.; Yu, W.Y.; Sun, H.Z.; Tam, P.K.H.; Chiu, J.F.; Che, C.M. Proteomic analysis of the mode of antibacterial action of silver nanoparticles. *J. Proteome Res.* **2006**, *5*, 916–924. [CrossRef] [PubMed]
63. Egger, S.; Lehmann, R.P.; Height, M.J.; Loessner, M.J.; Schuppler, M. Antimicrobial properties of a novel silver-silica nanocomposite material. *Appl. Environ. Microbiol.* **2009**, *75*, 2973–2976. [CrossRef]
64. Dizaj, S.M.; Lotfipour, F.; Barzegar-Jalali, M.; Zarrintan, M.H.; Adibkia, K. Antimicrobial activity of the metals and metal oxide nanoparticles. *Mater. Sci. Eng. C Mater.* **2014**, *44*, 278–284. [CrossRef]
65. Allahverdiyev, A.M.; Abamor, E.S.; Bagirova, M.; Rafailovich, M. Antimicrobial effects of TiO_2 and Ag_2O nanoparticles against drug-resistant bacteria and leishmania parasites. *Future Microbiol.* **2011**, *6*, 933–940. [CrossRef] [PubMed]
66. Archana, D.; Singh, B.K.; Dutta, J.; Dutta, P.K. Chitosan-PVP-nano silver oxide wound dressing: In vitro and in vivo evaluation. *Int. J. Biol. Macromol.* **2015**, *73*, 49–57. [CrossRef] [PubMed]
67. Yang, J.-Y.; Kim, H.-J.; Chung, C.-H. Photocatalytic antifungla activity against *Candida albicans* by TiO_2 coated acrylic resign denture base. *J. Korean Acad. Prosthodont.* **2006**, *44*, 284–294.

68. Jones, L.; Oshea, P. The electrostatic nature of the cell-surface of *Candida albicans*—A role in adhesion. *Exp. Mycol.* **1994**, *18*, 111–120. [CrossRef]
69. Carlile, M.J. The Photobiology of Fungi. *Annu. Rev. Plant Physiol.* **1965**, *16*, 175–202. [CrossRef]
70. Hill, E.P. Effect of light on growth and sporulation of *Aspergillus ornatus*. *J. Gen. Microbiol.* **1976**, *95*, 39–44. [CrossRef]
71. Kopke, K.; Hoff, B.; Bloemendal, S.; Katschorowski, A.; Kamerewerd, J.; Kuck, U. Members of the *Penicillium chrysogenum* velvet complex play functionally opposing roles in the regulation of penicillin biosynthesis and conidiation. *Eukaryot. Cell* **2013**, *12*, 299–310. [CrossRef]
72. Markowska-Szczupak, A.; Ulfig, K.; Morawski, A.W. Antifungal effect of titanium dioxide, indoor light and the photocatalytic process in vitro test on different media. *J. Adv. Oxid. Technol.* **2012**, *15*, 30–33. [CrossRef]
73. Markowska-Szczupak, A.; Wang, K.L.; Rokicka, P.; Endo, M.; Wei, Z.S.; Ohtani, B.; Morawski, A.W.; Kowalska, E. The effect of anatase and rutile crystallites isolated from titania P25 photocatalyst on growth of selected mould fungi. *J. Photochem. Photobiol. B* **2015**, *151*, 54–62. [CrossRef] [PubMed]
74. Raliya, R.; Biswas, P.; Tarafdar, J.C. TiO_2 nanoparticle biosynthesis and its physiological effect on mung bean (*Vigna radiata* L.). *Biotechnol. Rep.* **2015**, *5*, 22–26. [CrossRef] [PubMed]